Pramana – J. Phys. (2016) 87: 45
DOI 10.1007/s12043-016-1263-1

Various properties of the $0.6BaTiO_3$–$0.4Ni_{0.5}Zn_{0.5}Fe_2O_4$ multiferroic nanocomposite

RENUKA CHAUHAN* and R C SRIVASTAVA

Department of Physics, G.B. Pant University of Agriculture & Technology, Pantnagar 263 145, India
*Corresponding author. E-mail: renukagbpuat@gmail.com

MS received 10 June 2015; revised 3 December 2015; accepted 16 December 2015; published online 6 September 2016

Abstract. Structural, magnetic and ferroelectric properties of $0.6BaTiO_3$–$0.4(Ni_{0.5}Zn_{0.5}Fe_2O_4)$ multiferroic nanocomposite are presented here. The structural properties of the samples were studied by XRD and Raman spectroscopy which confirm the formation of $BaTiO_3$ (BTO) phase with a tetragonal perovskite structure and a small secondary spinel phase due to the ferrite content. The magnetic and electric orderings were investigated by vibrating sample magnetometer (VSM) and ferroelectric (P–E) loop tracer at room temperature. The inception of ferroelectric properties is due to barium titanate. The remnant polarization increases ∼5 times for the composite with $Ni_{0.5}Zn_{0.5}Fe_2O_4$ (NZFO) substitution compared to BTO. The remnant polarization is conducive for switching applications of multiferroic composite.

Keywords. Multiferroic; perovskite; spinel ferrite; vibrating sample magnetometer.

PACS Nos 75.85.+t; 77.84.−s

1. Introduction

The multiferroics acquire simultaneous magnetic and ferroelectric order and display magnetoelectric (ME) coupling consisting of the variation of dielectric/ferroelectric property (polarization, permittivity) under magnetic field and vice versa [1,2]. This property promotes the magnetoelectric energy conversion and thus is attractive for applications such as magnetic field probes, transducers, novel actuators, sensors, capacitive/inductive passive filters for communications, etc. Natural multiferroic single-phase compounds are very rare, and their magnetoelectric responses are either relatively weak or occur at temperatures too low for realistic applications. In contrast, multiferroic composites, which incorporate ferroelectric and ferri-/ferromagnetic phases, typically yield giant magnetoelectric coupling response above room temperature, which makes them fit for industrial applications. In the early 1990s, Newnham's group and Russian scientists prepared particulate ceramic composites of ferrites and $BaTiO_3/Pb(ZrTi)O_3$ by a conventional sintering process [3–6]. The sintered ceramic composites were much easier and cost-effective to fabricate in comparison to eutectic composites; and in addition, provided the opportunity to combine phases with widely different crystal structures. The main advantage of producing sintered ME composites are: the cheap and easy fabrication and the possibility to control the molar ratio of phase, grain size of each phase and densification.

In composite multiferroics, the coupling between the magnetic and electric order parameters is strain-mediated [7]. The known ME composite materials are in the form of ceramics, thin films and multilayers [8]. Lead zirconate titanate and barium titanate ($BaTiO_3$) are frequently used as ferroelectric (FE) components, whereas the ferrites are mostly used as magnetic module of the ME composites [9,10]. As the resistivity of the ferrite phase is not as good as that of FE materials, in such ME composites the percentage of ferrite phase is an important issue [11,12]. As the ferrite content increases, it becomes difficult to apply high voltages (as required for recording the FE hysteresis P–E loops) and therefore limit the applicability of these materials [13]. Adhlakha *et al* studied $Ni_{0.75}Zn_{0.25}Fe_2O_4$–$Ba(Ti_{0.85}Zr_{0.15})O_3$ composites and reported that the ME effect is maximum for 40 mol% of the ferrite phase [14]. Upadhyay *et al* and Gupta *et al* also studied the similar system with different compositions of $Ni_{0.5}Zn_{0.5}Fe_2O_4$ and $BaTiO_3$ [15,16].

Nickel zinc ferrite is a ferrimagnet below T_c (680 K) with a mixed spinel structure. The strength of magnetostriction reveals the cation distribution of NZFO showing mixed spinel structure [17]. The spinel structure belongs to a cubic crystal system with oxide anions arranged in a cubic close-packed lattice and metal cations tetragonally or octahedrally coordinated by the oxygen ions. It may be contemplated from previous studies that change in magnetic properties with the doping of ferroelectric material and change in ferroelectric properties with ferromagnetic material are not very well understood. Therefore, we studied the effect of BTO substitution on the magnetic properties of nickel zinc ferrite and effect of NZFO substitution on the ferroelectric properties of barium titanate.

2. Experimental

The nanoparticles of barium titanate and nickel zinc ferrite were prepared by solid-state reaction method. High-purity barium carbonate ($BaCO_3$) and titanium dioxide (TiO_2) were mixed together in 1:1 molar ratio and were grounded for 7 h with a mortar and pestle to prepare barium titanate. Wet mixing was done with ethanol to obtain a homogeneous powder mixture. This was followed by presintering in a furnace for 5 h at 600°C and then reground before final sintering at 1200°C for 5 h to get barium titanate. Nickel zinc ferrite was prepared by mixing NiO, ZnO and Fe_2O_3 in 0.5:0.5:1 molar ratio at similar conditions. Nickel zinc ferrite and barium titanate were used as preliminary precursors for the composite system. The composite was prepared by mixing barium titanate and nickel zinc ferrite powder in 60:40 molar ratio and finally sintered at 1200°C for 1 h. The dry mixtures were granulated by adding 4 wt% PVA binder, and pressed into pellets of 1–2 mm thickness and 10 mm diameter by applying a pressure of 10 MPa. The pellets were dried at 100°C for overnight and finally sintered in closed double crucibles at an optimum temperature of 1100°C for 4 h with a heating rate of 5°C/min and natural cooling rate. The X-ray diffraction (XRD) patterns were recorded using D8-Discover system of M/s Brucker (Germany), equipped with Cu-K_α radiation ($\lambda = 0.154$ nm) with a scan step of 0.002° and a counting time of 0.5 s/step in the range of $2\theta = 20-80°$. Raman spectroscopy measurements were carried out in the backscattering geometry using Labram-HR800 micro-Raman spectrometer equipped with Ar laser excitation source, 50× objective lens, an appropriate edge filter and a Peltier-cooled charge coupled device detector at room temperature. The magnetic measurements were carried out with 14 T PPMS-vibrating sample magnetometer at different temperatures. The P–E loop measurement was carried out using M/s Radiant Premier II system.

3. Results and discussion

Figure 1 shows the XRD patterns of $BaTiO_3$, $Ni_{0.5}Zn_{0.5}Fe_2O_4$ and BTO/NZFO composite. All the synthesized samples exhibit single phase as illustrated by XRD patterns. The XRD patterns of $BaTiO_3$ and $Ni_{0.5}Zn_{0.5}Fe_2O_4$ are perfectly matched with the reference XRD patterns (JCPDS, PDF No. 79-2264 and 01-072-6799 respectively).

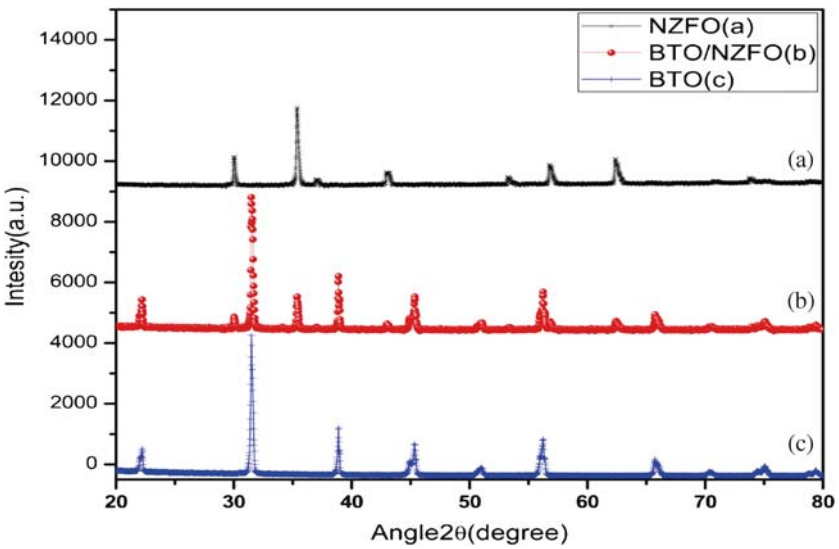

Figure 1. XRD patterns of BTO, NZFO and BTO/NZFO nanocomposite.

The XRD pattern of the composite is observed as BTO phase with tetragonal perovskite (space group = *P4mm*) and a small ferrite phase with spinel structure (space group = *Fd3m*). The crystallite size for both $BaTiO_3$ and $Ni_{0.5}Zn_{0.5}Fe_2O_4$ phases were determined using Scherrer's equation. These are in the range of 40–50 nm.

Figure 2 shows the Raman spectra of the prepared composite along with pure BTO and NZFO ceramics for comparison. The Raman spectrum of BTO shows a broad peak at 259 cm^{-1} [E(TO)], a sharp peak at 304 cm^{-1} [E(TO+LO)], an asymmetric peak near 518 cm^{-1} [E(TO)] and a broad peak at 715 cm^{-1} [E(LO)], where the mode assignment is given inside the square brackets. The present Raman data of BTO match excellently with the literature for bulk BTO [18].

The Raman spectrum of NZFO exhibits sharp modes at 333 cm^{-1}, 480 cm^{-1} and 687 cm^{-1} corresponding to the first-order Raman active modes of $A_{1g}+E_g+T_g$. Apart from these modes, one broad peak at 650 cm^{-1} is observed for the NZFO. The origin of this broad peak in NZFO is reported to be due to the large mass difference between Ni^{2+}, Fe^{2+} and Zn^{2+} [19,20]. The Raman spectra of composites mainly consist of peaks corresponding to BTO phase. However, the signature of NZFO phase is also seen in the Raman data of the composite. For example, the Raman mode of BTO at 518 cm^{-1} of the composite sample is not symmetric on the higher wave-number side, because of the presence of a mode of NZFO occurring at 482 cm^{-1}. Hence, the XRD and Raman data confirm the formation of biphase composites consisting of NZFO as ferrimagnetic and BTO as ferroelectric phase in the prepared composite samples.

Figure 3 shows magnetization as a function of field (*MH* curve) for the composite and pure NZFO at 10 and 300 K. The magnetic signal basically comes from the NZFO phase present in the samples. In the case of the composite, the saturation magnetization, coercivity and remnant magnetization are found to be less than for pure NZFO. The magnetization is not completely saturated even up to the field of 50 kOe. Hence, saturation

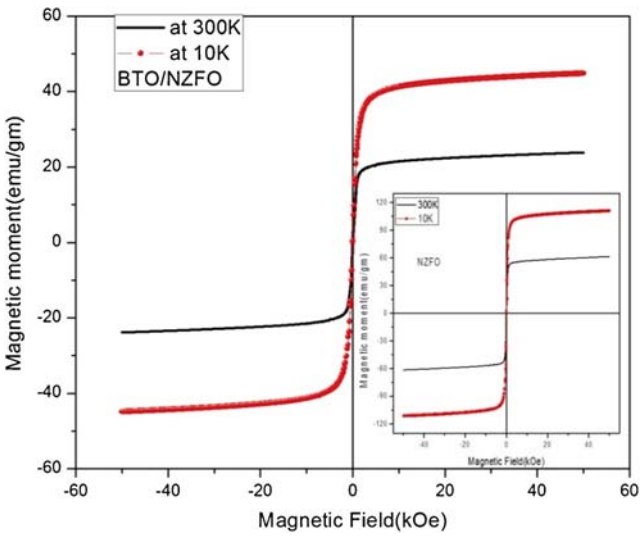

Figure 3. *M–H* curves for NZFO (in the inset) and BTO/NZFO composites at 10 and 300 K temperatures.

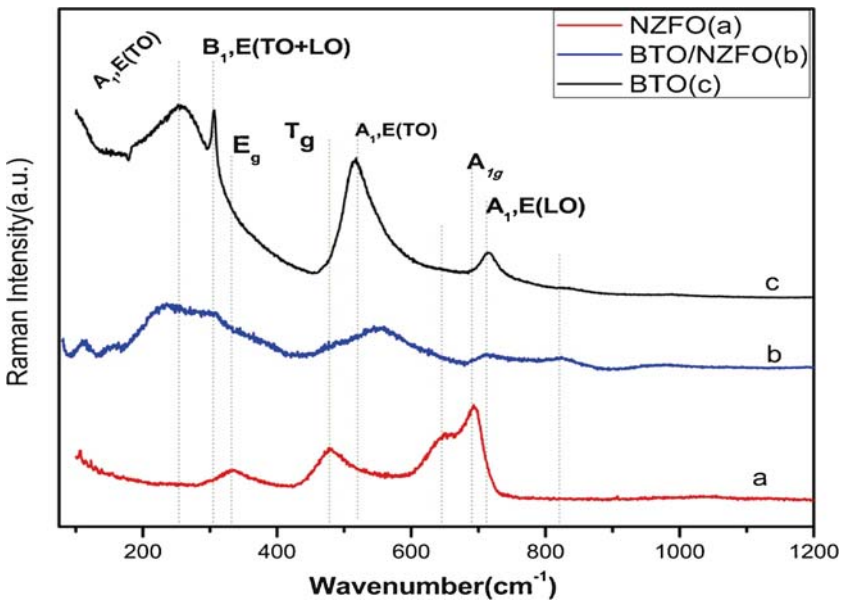

Figure 2. Raman spectra of BTO, NZFO and BTO/NZFO nanocomposite. Vertical dotted lines show the mode positions corresponding to BTO and NZFO phases respectively.

magnetization (M_s) is evaluated using the following equation:

$$M = M_s(1 - a/H).$$

In the high-field region, the plot between M and $1/H$ is a straight line whose intersection with $1/H = 0$ axis gives the value of M_s. The saturation magnetization thus obtained is 114 and 45 emu/g at 10 K, 65 and 24 emu/g at room temperature for NZFO and the composite respectively. The magnetic moment is reduced in comparison with pure nickel ferrite (∼70 emu/g). In pure NZFO, the spontaneous magnetization originates from unbalanced antiparallel spin (ferromagnetic character) giving rise to small values of coercivity and saturation magnetization.

Higher magnetization values are characteristic to the samples at 10 K. It is observed that coercivity is nearly zero for all the samples at 10 K, but at room temperature it varies from 84 Oe to 33 Oe. Remnant magnetization also shows similar pattern as coercivity at 10 K and at room temperature. High saturation magnetization is due to the magnetic behaviour of nickel zinc ferrite, which is related to cation distribution and Neel theory of ferrimagnetism [17].

The decrease in magnetization value of BTO/NZFO composite clearly demonstrates the dilution effect of the incorporation of the nonmagnetic phase. Once the diphase composite is obtained, it is important to know if the intrinsic properties of the magnetic and ferroelectric phases are maintained, without major changes in the interaction mechanisms due to the foreign phase, particularly, the magnetic properties. If the presence of BTO phase does not cause intimate change in magnetic interactions, dilution effect in the magnetic property is expected. The magnetic property of the composite is due to the ferrite phase [21–24]. The presence of the nonmagnetic perovskite phase and the interface effects are expected to influence the magnetic properties in the ceramic composites by changing the distribution of the magnetic ions and their spin orientation leading to the change in magnetic interactions.

The magnetic characteristic of the composite at room temperature is quite similar to that at low temperature (10 K), the major difference being the reduction of saturation magnetization for the sample with rise in temperature. The lower magnetization may be due to a better segregation of the magnetic phase by the nonmagnetic one in the core–shell composite, which diminishes the effect of magnetostatic interactions. Thus, the observed values for the magnetization at a given field and at saturation are expected to result from the microstructural differences of the composites. Some more subtle distinction might also result from particular nanoscale characteristics (interfaces, interconnectivity) as formerly found in other $BaTiO_3$–$Ni_{0.5}Zn_{0.5}Fe_2O_4$ composites by a detailed thermomagnetic investigation [24].

Further temperature-dependent magnetization (M–T) measurements were carried out for all the samples at 5 T in field-cooled (FC) and zero-field-cooled (ZFC) conditions as shown in figure 4. The FC and ZFC magnetization curves show a divergence at low temperature. The irreversibility temperature, which is considered as the point where the ZFC and FC curves begin to separate, is higher for the composite. The irreversible temperature is found to be 279 K for pure nickel zinc ferrite while it is greater than 300 K for the BTO/NZFO composite. The ZFC curve exhibits a broad peak and the peak temperature is 45 K for pure NZFO and 62 K for the composite.

The ferroelectric properties were observed in RT ferroelectric (P–E) loop at 50 Hz as shown in figure 5. The saturation polarization (P_s) has higher value for composite than for pure barium titanate, but the leakage current contribution increases with ferrite content. The P–E loop indicates weak ferroelectricity with higher remnant polarization for the composite. The poor hysteresis may be due to the high leakage current. It is found that the width of the P–E loop decreases with increase in frequency. The inception of ferroelectricity in the present system may be attributed to the structural distortion from a high symmetry phase that removes the centre of symmetry and allows electric polarization. The values of dielectric constant at 100 kHz and at room temperature for BTO, NZFO and BTO/NZFO composites were found to be 2550, 400 and 1050 respectively.

The positive curvature of the P–E loop indicates that the contribution of leakage current is less in the case of pure BTO. The saturation polarization is also less for BTO, because of porosity in the pellets. However, for composite sample it is observed that remnant polarization P_r increases continuously even after transition temperature (T_{C-FE}), because the leaky behaviour of P–E loop is increased as the temperature is increased. Higher value of remnant polarization is useful for switching applications. The leaky behaviour is mainly due to the presence of ferrite phase in the composites and as the fraction of NZFO increases, the contribution of leakage current also increases. Therefore, in such samples the P–E loop data may not truly give the value of true FE polarization, i.e., switched charge density.

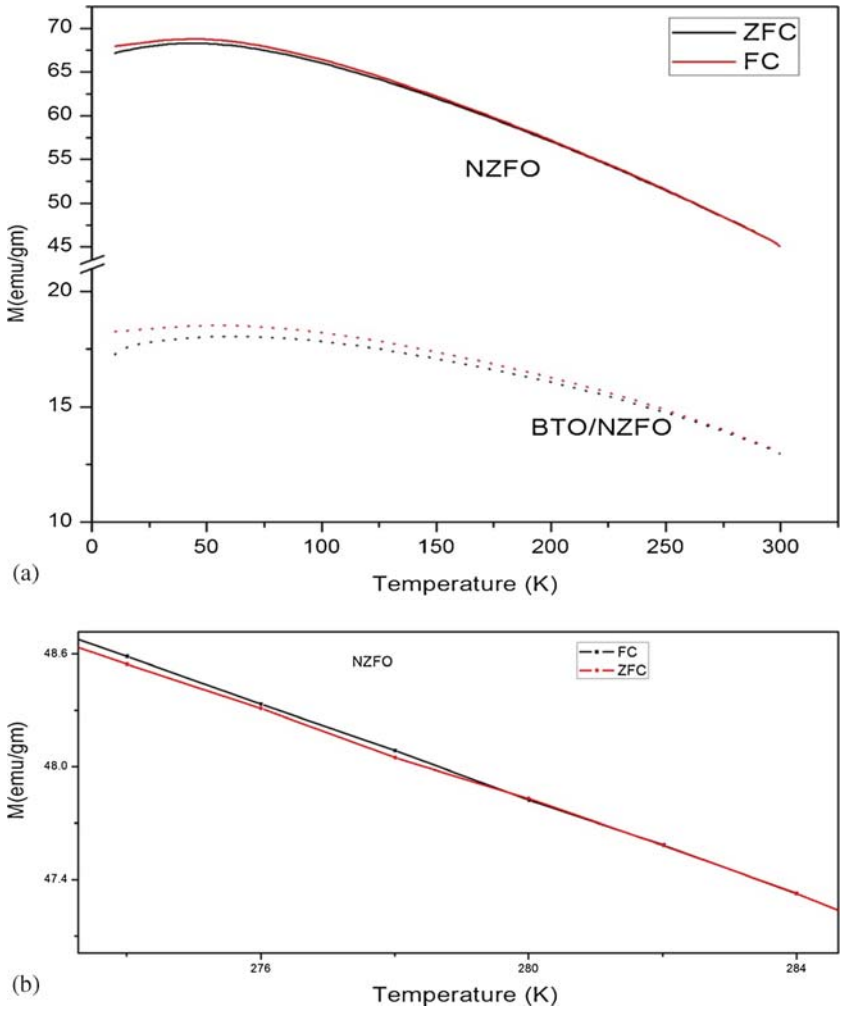

Figure 4. (**a**) Temperature-dependent magnetization (M–T) curves for NZFO and BTO/NZFO composite at an applied magnetic field of 5 T and (**b**) the enlarged view of M–T curve for irreversible temperature.

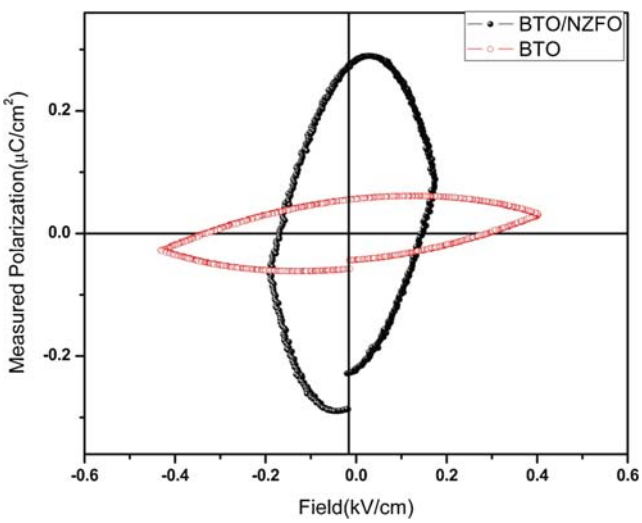

Figure 5. Room temperature (RT) P–E for pure BTO and BTO/NZFO composite at 50 Hz.

4. Conclusion

The multiferroic BTO/NZFO nanocomposite was prepared by solid-state reaction method. XRD confirms the pure phase of the tetragonal perovskite structure of BTO and cubic spinel structure of NZFO. The presence of biphase is also confirmed from the Raman spectroscopy measurements. Magnetic and electric orderings at room temperature is confirmed by recording the M–H and P–E loops. The FC–ZFC magnetization curves show that the irreversible temperature of the composites is above 300 K. It is concluded that the analogous structural differences, due to the ferrite concentration, leads to changes in the magnetic and ferroelectric properties of composites.

Acknowledgements

The authors are thankful to Dr V Ganesan for providing the facilities of UGC–DAE–CSR Indore Centre.

Moreover, thanks are also due to Drs Alok Banerjee, V Sathe, V R Reddy and Mukul Gupta for their keen interest and suggestions in VSM, Raman, P–E and XRD measurements, respectively.

References

[1] H Schmid, *Ferroelectrics* **162**, 19 (1994)
[2] A J Freeman and H Austin, *Magnetoelectric interaction phenomena in crystals* edited by A J Freeman and H Schmid (Gordon and Breach Science Publishers, Newark, New York, 1975) pp. 181–194
[3] G Harshe, J P Dougherty and R E Newnham, *Int. J. Appl. Electromagn. Mater.* **4**, 145 (1993)
[4] S Lopatin, I Lopatin and I Lisnevskaya, *Ferroelectrics* **162**, 63 (1994)
[5] T G Lupeiko, I V Lisnevskaya, M D Chkheidze and B I Zvyagintsev, *Inorg. Mater.* **31**, 1245 (1995)
[6] M I Bichurin, I A Kornev, V M Petrov and I Lisnevskaya, *Ferroelectrics* **204**, 289 (1997)
[7] S K Mandal, G Sreenivasulu, V M Petrov and G Srinivasan, *Appl. Phys. Lett.* **96**, 192502 (2010)
[8] C W Nan, M I Bichurin, Shuxiang Dong, D Viehland and G Srinivasan, *J. Appl. Phys.* **103**, 031101 (2008)
[9] J Huang, P Du, L Hong, Y Dong and M Hong, *Adv. Mater.* **19**, 437 (2007)
[10] G Sreenivasulu, V Hari Babu, G Markandeyulu and B S Murty, *Appl. Phys. Lett.* **94**, 112902 (2009)
[11] G Srinivasan, C P DeVreugd, C S Flattery, V M Laletsin and N Paddubnaya, *Appl. Phys. Lett.* **85**, 2550 (2004)
[12] L Mitoseriu, I Pallecchi, V Buscaglia, A Testino, C E Ciomaga and A Stancu, *J. Magn. Magn. Mater.* **316**, e603 (2007)
[13] Y HuiZheng, X Dong, W Wang, G Weng, N Han and P D Ma, *Angew. Chem. Int. Ed.* **48**, 8927 (2009)
[14] Nidhi Adhlakha and K L Yadav, *Smart Mater. Struct.* **21**, 115021 (2012)
[15] Sanjay Kumar Upadhyay and V Raghavendra Reddy, *J. Appl. Phys.* **113**, 114107 (2013)
[16] Gupta Arti, A Huang, Santiranjan Shannigrahi and Ratnamala Chatterjee, *Appl. Phys. Lett.* **98**, 112901 (2011)
[17] J Samuel Smart, *Am. J. Phys.* **23**, 356 (1955)
[18] R Naik, J J Narzarko, C S Flattery, U D Venkateswaran, V M Nayak, M S Mohammed, G W Auner, J V Mantese, N W Chubring, A L Micheli and A B Catalan, *Phys. Rev. B* **61**, 11367 (2000)
[19] P S Dobal *et al*, *J. Appl. Phys.* **89**, 8085 (2001)
[20] Mohit Kumar, S K Rout, S Parida, G P Singh, S K Sharma, S K Pradhan and I Won Kim, *Physica B* **407**, 935 (2012)
[21] S W da Silva, F Nakagomi, M S Silva, A Franco Jr, V K Garg, A C Oliveira and P C Morais, *J. Nanopart. Res.* **14**, 798 (2012)
[22] S Narendra Babu *et al*, *J. Appl. Phys.* **109**, 07D904 (2011)
[23] N Ponpandian, A Narayanasamy, C N Chinnasamy, N Sivakumar, J-M Greneche, K Chattopadhyay, K Shinoda, B Jeyadevan and K Tohji, *Appl. Phys. Lett.* **86**, 192510 (2005)
[24] L Mitoseriu, I Pallecchi, V Buscaglia, A Testino, C E Ciomaga and A Stancu, *J. Magn. Magn. Mater.* **316**, e603 (2007)